Diffusion-weighted imaging and diffusion tensor imaging of the heart *in vivo*: major developments

Weronika Mazur[1], Artur T. Krzyżak[2], Franciszek Hennel[3]

[1]Faculty of Physics and Applied Computer Science, AGH University of Science and Technology, Krakow, Poland
[2]Faculty of Geology, Geophysics and Environmental Protection, AGH University of Science and Technology, Krakow, Poland
[3]Institute for Biomedical Engineering, University of Zurich and ETH Zurich, Zürich, Switzerland

Abstract

Diffusion-weighted magnetic resonance imaging (DWI) is a powerful diagnostic tool. Contrast in DWI images is dictated by the differences in diffusion of water in tissues, which depends on the tissue type, hydration and fluid composition. Therefore DWI can differentiate between hard and soft tissues, as well as visualize their condition, such as edema, necrosis or fibrosis. Diffusion tensor imaging (DTI) is a DWI technique which additionally delivers information about the microstructure. In cardiovascular applications DWI/DTI can non-invasively characterize the acute to chronic phase of the area at risk and microstructural dynamics without the need to use contrast agents. However, cardiac DWI/DTI differs from other applications due to serious anatomic and technologic challenges. Over the years, scientists have stepped up overcoming more and more advanced obstacles associated with complex 3D myocardial motions, breathing, blood flow and perfusion. The aim of this article is to review milestone technologic advances in DWI/DTI of the heart *in vivo*. The discussed development begins with the adjustment of the diffusion imaging block to the electrocardiogram-based most quiescent phase, next considers different pulse sequence designs for first-, second- and higher-order motion compensation and SNR improvement, and ends up with prospects for further developments. Reviewed papers show great progress in this research area, but the gap between the scientific development and common clinical practice is tremendous. Cardiac DWI/DTI has promising clinical relevance and its addition to routine imaging techniques of patients with heart disease may empower clinical diagnosis.

Key words: cardiac diffusion-weighted imaging, cardiac diffusion tensor imaging, *in vivo* diffusion-weighted magnetic resonance imaging (DWI), *in vivo* diffusion tensor imaging (DTI).

Introduction

The ability of magnetic resonance imaging (MRI) to quantify molecular diffusion provides insight into microscopic features of materials and biological tissues at a scale much finer than the image resolution. Diffusion MRI has become a standard tool to grade ischemic lesions and tumors in the brain [1–3] and its applications to study diseases of other organs are gaining ground [4]. A particularly powerful feature of diffusion MRI is the sensitivity to directional properties (anisotropy) of the medium, which opens ways to visualize axonal tracts in the brain [5] and the structure of myocytes in muscles [6] (Table I). Diffusion sensitization is achieved by combining MRI pulse sequences with strong motion-encoding gradient pulses, which cause signal attenuation in the presence of random Brownian motion of water molecules.

At the same time, diffusion-sensitizing gradients lead to signal phase shifts in the case of coherent motion of all spins included in an image voxel. This effect constitutes a major challenge for diffusion MRI of moving organs (Table II).

Diffusion-weighted imaging (DWI) of a heart is particularly challenging due to the scale of the cardiac motion and blood flow, which surpasses the diffusional displacements by a few orders of magnitude and has an enormous impact on the signal phase, up to the effect of complete signal cancellation. Blood flow may cause diffusion coefficient overestimation, while respiration and cardiac pulsation additionally make it difficult to register a signal coming from the heart (Table II). Hence, different approaches have been developed over the years to improve DWI of the heart and enable its quantitative anal-

ysis. Immediately after the introduction of the diffusion tensor imaging (DTI) concept for the characterization of anisotropic media, attempts were made to apply it to the heart. However, despite the achievement of many milestones, DTI of the heart *in vivo* remains challenging. This paper aims to review the major methodological steps taken towards accurate DWI and DTI of the human heart *in vivo*.

The first DWI of the human heart *in vivo*

The first attempt at the DWI of a human heart *in vivo* was performed by Edelman *et al.* [7] in 1994. The main advantage of applying DWI seen by the authors was the possibility to obtain structural information about the myocardium, such as fiber orientation or compartmentalization. They proposed to address the difficulty of a bulk heart movement by the first application of an echo planar imaging (EPI) method that is synchronized with the cardiac cycle (Table III). At the same time, they applied a stimulated spin echo (STE) pulse sequence with a breath hold.

Breath holding prevents the respiratory movement influencing diffusion measurements. STE relies on the application of three 90° radiofrequency (RF) pulses. The first two are separated by a diffusion-sensitizing magnetic field gradient (or dephasing gradient) and the second one is followed by the diffusion time. After that, the third RF pulse and subsequently the second gradient (or rephasing gradient) are applied and the diffusion-weighted signal (echo) is encoded (Figure 1 A). During diffusion time magnetization is stored along the main magnetic field, B_0, which makes it sensitive to T_1 rather than T_2 relaxation (see Figure 1 for comparison of spin echo and stimulated echo pulse sequences). This enables a longer

Table I. Diffusion-weighted imaging (DWI)/diffusion tensor imaging (DTI) of the heart – an important research target: Why?

- Non-invasive information about myocardial microstructure (histology quality [1]).
- Can complement the area at risk diagnosis in the acute and subacute phase (Figure 3).
- An alternative for patients with contraindications to gadolinium use (Figure 3).
- Can reflect macroscopic cardiac functions and help to understand the link with cellular contraction.
- Unique insight into microstructural dynamics.

interval between magnetic field gradients to be used without the total loss of a signal, and long enough to use electrocardiographic (ECG) gating.

The technique proposed by Edelman et al. relied on two gate triggers set after some time (delay) after two R-waves (called double gating, see Figure 2 A). The diffusion (Δ) and echo times (*TE*) were equal to the R-R interval and 42 ms, respectively, while gradient duration was 10 ms. The *b*-value achieved for such time conditions was 395 s mm^{-2}, while for the standard approach with rectangular gradient pulses the *b*-value is calculated from,

$$b = (\gamma \times \delta \times G)^2 \times (\Delta - \frac{\delta}{3})$$

where γ is gyromagnetic ratio, δ is diffusion gradient pulse duration, *G* is diffusion gradient amplitude and Δ is two diffusion gradient pulses' separation time (Figure 1). In order to assure the same cardiac cycle during dephasing and rephasing gradients, trigger delays have to be equal. Spin-echo EPI (SE-EPI) proved to be insufficient for obtaining artifact-free DWI, while only very low *b*-values (~20 s mm^{-2}) enabled the registration of a signal of a heart.

Development of DTI of the heart *in vivo*

Desensitization to motion effects in DTI

The first full diffusion tensor in vitro and in vivo with strain measurements

Myocardial function can be associated with the size of chambers, inotropic stimulus, but also the heart muscle fiber architecture. Diffusion anisotropy reflects the local structural orientation of the tissue [8], which led Garrido *et al.* [9] to determine it in order to obtain fiber archi-

Table II. Fundamental challenges in diffusion-weighted imaging of the heart

Anatomical
- Proximity of lungs to the heart, resulting in image distortions due to differences between magnetic susceptibilities of water and air.
- Image distortions and hindered quantitative DWI/DTI analysis caused by significant flow in large blood vessels entering the heart.
- Myocardium movements in relation to cardiac pulsation and respiration (huge in relation to diffusion length) causing significant (no-diffusion-related) signal losses.

Technological
- Difficulty of applying diffusion encoding gradients in the same cardiac phase in different cycles, especially in arrhythmic patients.
- Complex 3D motions of the heart, which are hard to compensate.
- Short transverse relaxation time, T_2, imposing short echo time in order to avoid excessive signal attenuation.
- High diffusion weightings, *b*-values, are hard to obtain due to limited diffusion time and gradient length in the static cardiac phase as well as gradient amplitude available in clinical setting.
- Decreased signal-to-noise ratio for higher-order motion compensation methods and stimulated spin echo pulse sequences.

Table III. Milestone advances in DWI/DTI of the heart

- Application of echo-planar imaging.
- Development of methods for the first-, second- and higher-order motion compensation.
- Encoding diffusion during a single heartbeat (no need for breath holding).
- Application of spin-echoes for cardiac diffusion measurements.
- Identification (and effective use of) sweet spots for strain-free diffusion imaging.
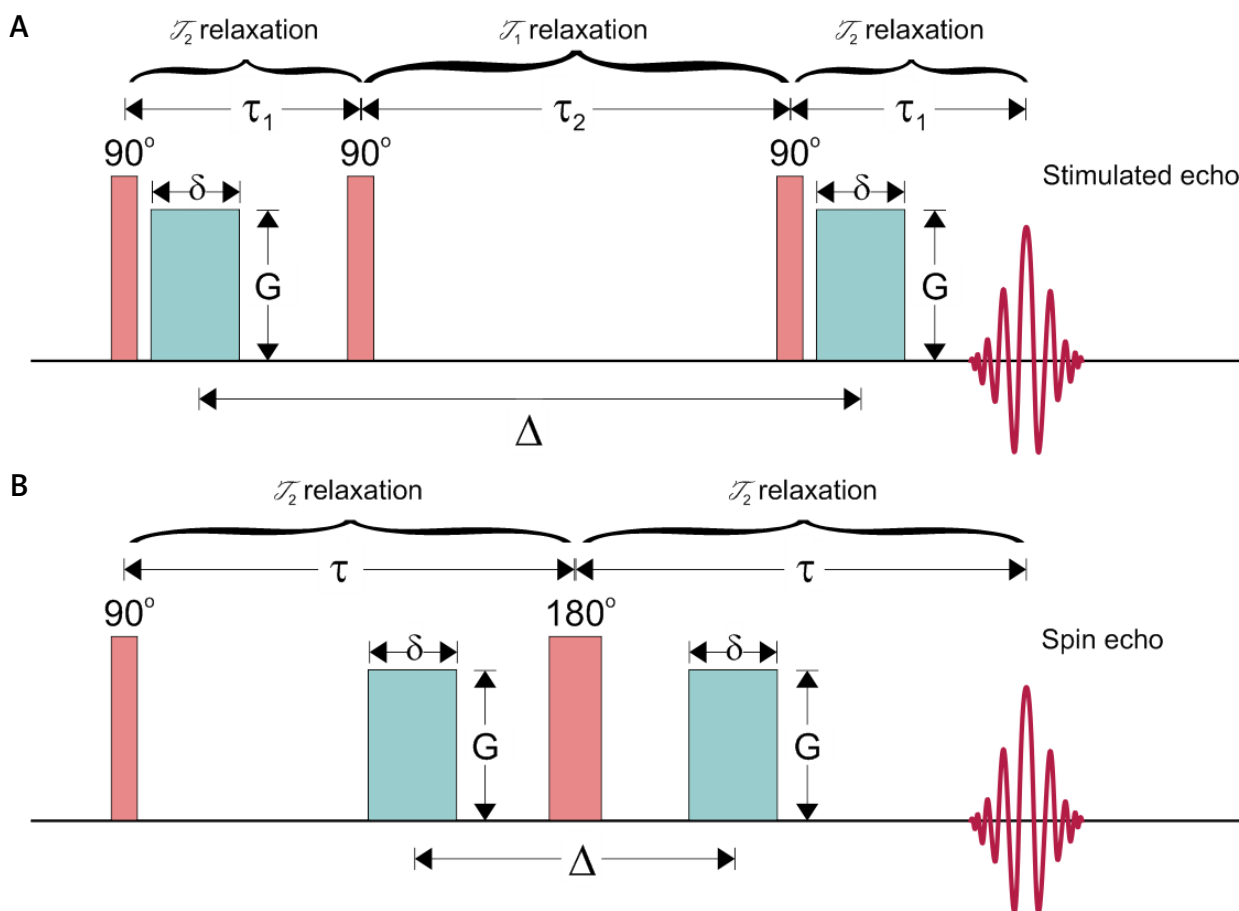
Figure 1. Stimulated (STE; **A**) and spin (SE; **B**) echo pulse sequences for diffusion encoding with marked dominating relaxation processes in given intervals. 90° and 180° blocks are radiofrequency (RF) pulses that flip magnetization to transversal plane and invert spin phases, respectively, τ_1 and τ_2 are separation times of the first two and last two 90° RF pulses, τ is 90° and 180° pulses' separation time, green blocks are diffusion gradient pulses with amplitude *G*, duration δ and separation Δ. Note: that registered signal, $S \propto \exp(-bD) \times \exp\left(-\dfrac{TE}{T_2}\right) \times \exp\left(\dfrac{\Delta}{T_1}\right)$, in the STE diffusion signal is mostly sensitive to T_1 relaxation ($\tau_2 \gg \tau_1$), while mostly sensitive to T_2 relaxation in SE ($2\tau > \Delta$)

tecture of the rat's myocardium *in vitro*. Real anisotropy of the tissue required assessment of a full diffusion tensor. Even though this first attempt of DTI was performed on the intact heart, it delivered preliminary information about diffusion anisotropy in the myocardium.

The *in vivo* implementation of DTI was introduced by Reese *et al.* in 1995. They adopted the ECG-double-gated STE pulsed field gradient (PFG) technique proposed by Edelman *et al.* as efficient for motion compensation, in which they recognized another effect of material strain upon the NMR spin physics. To correct for the myocardial deformation at each location across the whole cardiac cycle, they assumed linear phase deformation conjugated with the stretch tensor of a material. The true diffusion tensor could be determined from the apparent one and a strain history obtained independently by NMR methods. Besides the full diffusion description and informa-

tion about its anisotropy, the proposed method provided a new tool for studying the dynamics of fiber architecture *in vivo* (Table I). For example, the authors demonstrated that with the application of their methodology it was possible to compare strain rate and wall thickness (represented by the highest eigenvalue) distribution widths, which confirmed the hypothesis of transmural equalization of fiber shortening relative to wall thickening.

Strain-corrected DTI in vivo without strain history measurements

Even though having significant capabilities, the method proposed by Reese *et al.* [10] for strain correction is complex and time-consuming, leading to reduced SNR and increasing the risk of systematic errors (Table II). Indeed, dilation and contraction can have a relevant influence on diffusion coefficients, but these processes can be
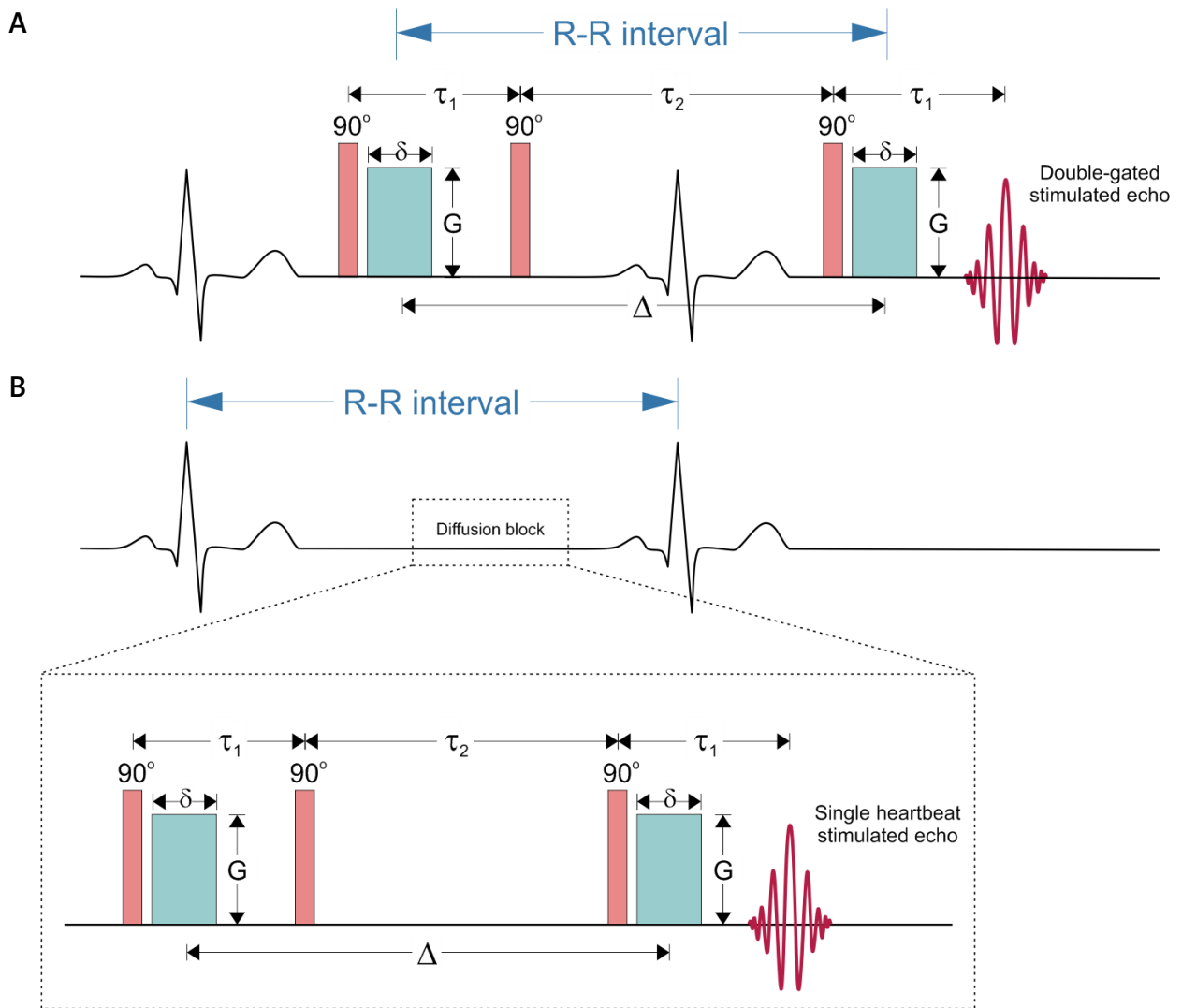
Figure 2. Schematic representation of double-gated stimulated echo (STE) pulse sequence (**A**) in comparison to single heartbeat STE (**B**) for diffusion measurement. 90° is the radiofrequency (RF) pulse that flips magnetization to the transversal plane, τ_1 and τ_2 are separation times of the first two and last two RF pulses, green blocks are diffusion gradient pulses with amplitude *G*, duration δ and separation Δ, which is a diffusion time considerably smaller than the R-R interval for the single heartbeat encoding (Table III)

omitted if diffusion is encoded in the characteristic moments defined by Tseng *et al.* and called "sweet spots" [11] (Table III). They developed an approach of finding sweet spots by relying on a very important observation that myocardial strains are highly synchronous and can be accurately approximated by the periodic time-dependent scaling of a fixed strain image. If this scaling fulfils certain requirements at a given moment in time, then the measured diffusion tensor is a true one. As the authors pointed out, periodicity and continuity of scaling function confirm the existence of at least two sweet spots, which in a cardiac cycle are located in mid-ejection and in mid-filling. Later, it was shown that the systolic phase has advantages over the diastolic phase, mainly the thicker myocardial wall with smaller requirements for spatial resolution and lower sensitivity to heart-rate variations [12].

Despite the two key approximations made, that diffusion is linearly dependent on strain and that strain history can be obtained without local material tracking as proposed by Reese *et al.* [10], the associated error for diffusion measurements is less than 6% and 2%, respectively. Sweet point miss-targeting leads to the error rate of 0.4% per millisecond of time shift. The method proved to be effective for obtaining reliable DTI data of a beating heart with acceptable error and provides reproducible fiber orientations (Table III).

Flow-compensated strain correction

Concerned about the possibility of occurrence of various cardiac motions unrecognized in strain measurements or other unanticipated mechanisms that can influ-
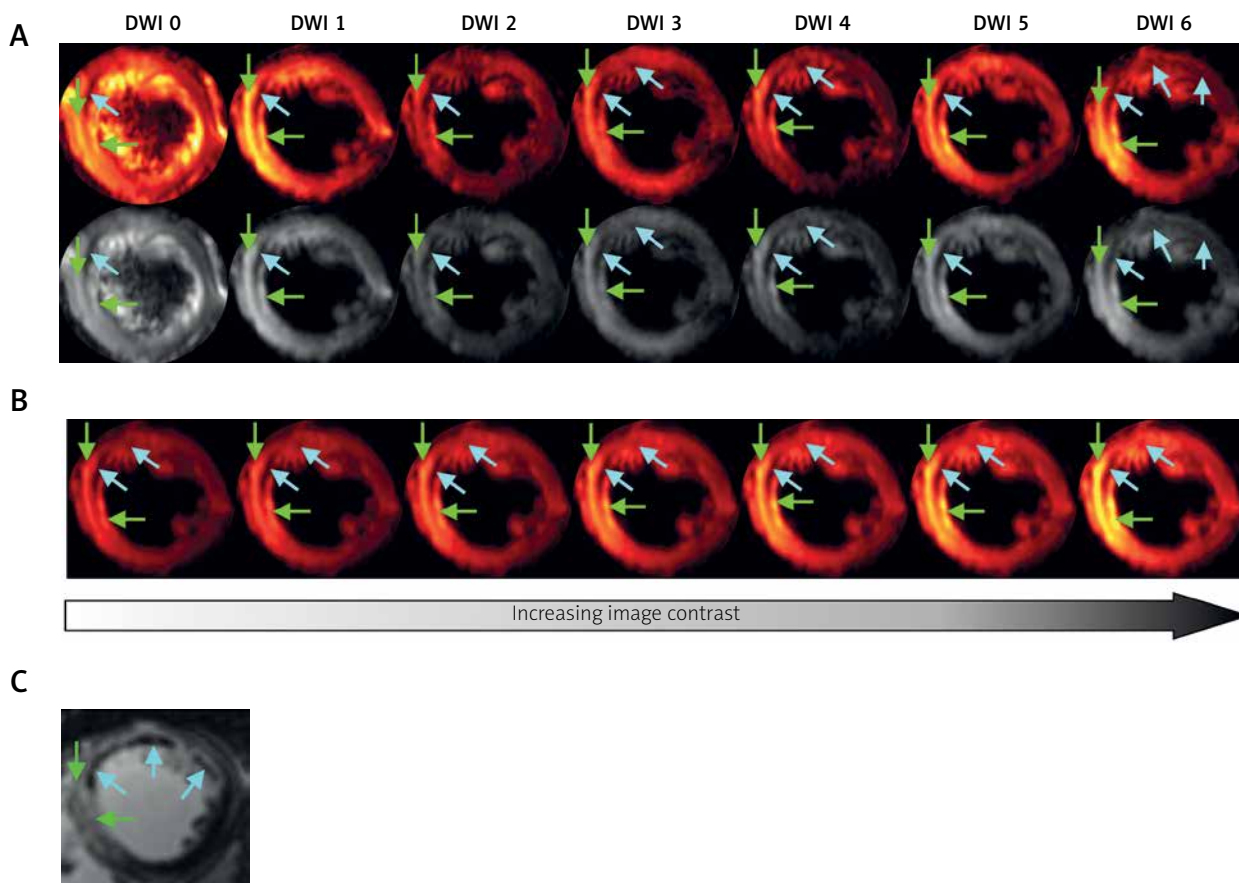
Figure 3. Images from patient with AMI (5 days after pPCI) obtained by using SE-EPI DTI sequence with details given previously [29]. A, B – and T_1-weighted imaging with late gadolinium enhancement. **A** – Raw DWI images for $b = 0$ s mm^{-2} (DWI 0) and for six non-collinear diffusion gradient directions (DWI 1-6) required for diffusion tensor calculation: hot scale (upper row) and grey scale (bottom row); **B** – method for visualization of damage zones with different severity by using increasing image contrast; **C** – T_1-weighted image with late gadolinium enhancement. Green arrows indicate infarction area – hyperintense spots in comparison to remote tissues, while blue arrows indicate microvascular obstruction – signal loss

ence diffusion experiments, Dou *et al.* presented another method for strain correction [13]. It relies on the application of two bipolar diffusion-sensitizing gradients, while the bipolarity of the second one (after the second R-wave) provides flow compensation. Bipolar diffusion gradients per se produce diffusion sensitization only during their duration, which was reported to be about 30 ms [13]. It is shorter than the myocardium contraction time, which makes the diffusion measurements strain-insensitive. This is contrary to unipolar diffusion gradients, for which diffusion sensitization occurs during the whole cardiac cycle (up to the end of the rephasing, unipolar gradient), which makes the measurements strain-sensitive.

The proposed methodology has the advantage of encoding diffusion only over a single cardiac phase (Figure 2 B). During a bipolar gradient pulse strain effects can result from a residual phase modulation if the gradient lobes are not the same shape, but remain negligible. Due to limitation of the gradient strength for clinical appli-

cations, obtaining the desired *b*-value (300–400 s mm^{-2} based on previous papers) imposes long diffusion-encoding times. This increases *TE* and reduces SNR and spatial resolution, which can be improved by the application of stronger magnetic field gradients (Table II).

Introduction of SE-EPI for *in vivo* cardiac DTI

Single-shot, double-gated EPI, after being proposed by Edelman *et al.* [7], became a powerful tool for the diffusion measurements of the beating heart (Table III). Its choice was obvious due to the ability of rapid data acquisition for the entire image. In combination with STE, it makes the diffusion measurements almost insensitive to bulk motion. Eventually, by encoding e.g. at the mid systole of the cardiac cycle by using bipolar gradients, it seems that diffusion measurement reflects reasonably (within acceptable error level) the undisturbed diffusion in the myocardium within two heartbeats (diffusion time is equal to R-R interval). However, STE-EPI has a major
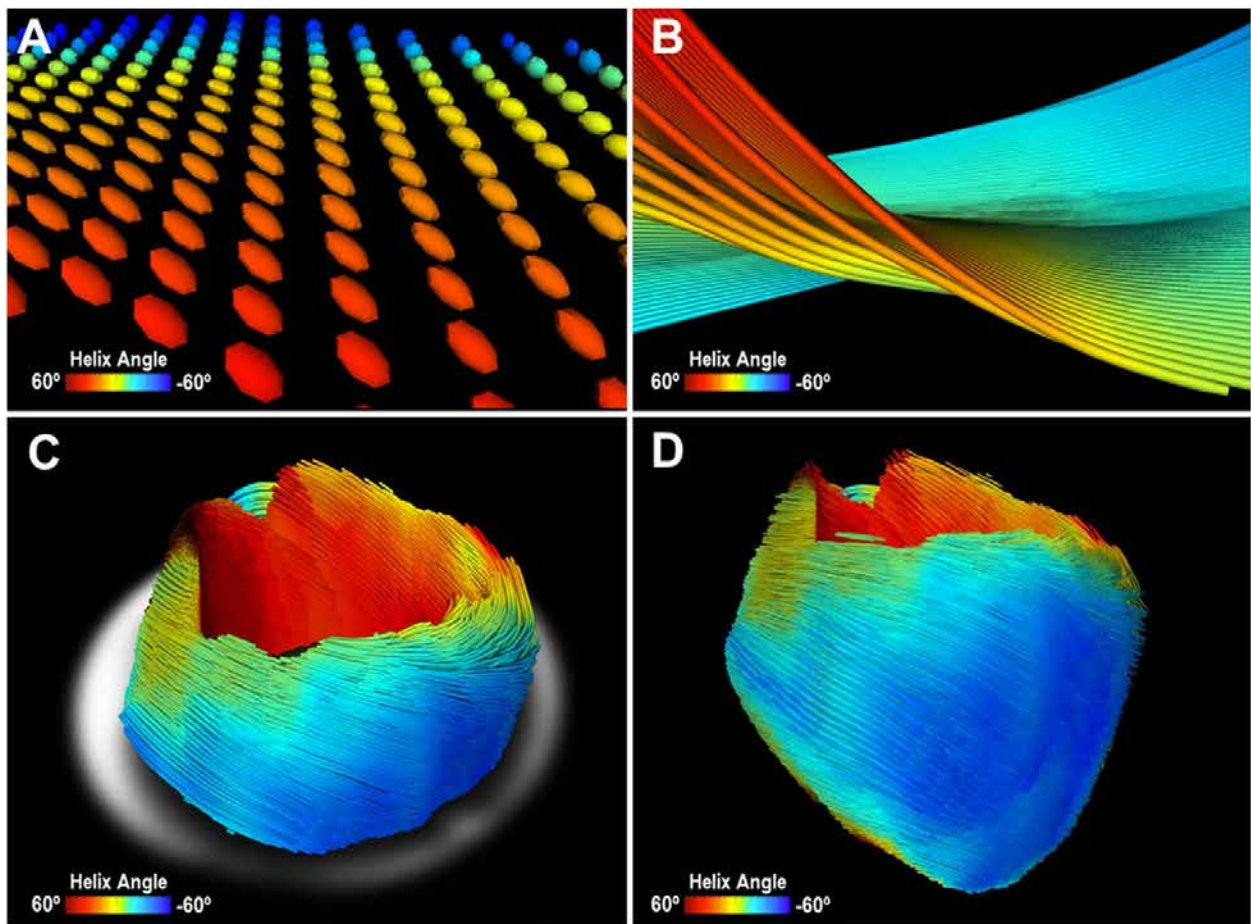
Figure 4. Unmodified Figure 4 from: Three-dimensional cardiomyocytes structure revealed by diffusion tensor imaging and its validation using a tissue-clearing technique; "Representative image of mouse heart DTI. **A** – Zoomed-in view of 3D diffusion tensors calculated at each voxel in the short-axis plane. Orientation of the anisotropy of the diffusion tensor is conventionally assumed to be parallel to the underlying cardiomyocytes orientation. Diffusion tensors are color-coded based on the calculated helix angle. **B** – Zoomed-in view of 3D cardiomyocytes tracking in the myocardium. **C** – Reconstructed cardiomyocytes above the mid-left ventricle on a short-axis plane. **D** – 3D tractography of the helix angle of a mouse heart visualizes the helical structure of the cardiomyocytes twisting around the left ventricle." By Lee *et al.* [32] licensed under CC BY 4.0 [34]

drawback over the SE pulse sequence of a very low SNR [12] (Table II). Gamper *et al.* found that SNR in flow-compensated (double bipolar diffusion gradients) SE-EPI can be more than 8-fold higher than in STE [12]. In spite of this fact, they showed some requirements that the diffusion experiment by using SE must fulfil.

Simulations of phase distribution of moving spins within the myocardium revealed significant phase gradients if an inappropriate voxel size is chosen [12]. It was shown that in order to obtain an undistorted image of the myocardium, one has to choose as far as possible some specified voxel size for a given *b*-value and systole phase. For uncompensated flow in the mid-systole this required resolution is very high (< 0.5 mm^2) for *b* = 200–600 s mm^{-2} and hard to obtain. Using bipolar rephasing gradient leads, besides flow compensation, to reduction of the required resolution to 4–5 mm^2 for the same *b*-value range.

The other important modification for cardiac diffusion imaging that was proposed by Gamper *et al.* is the application of the inner volume imaging method reported by Feinberg *et al.* [14] in the early years of MRI. This method is also called reduced field of view (FOV) and briefly relies on reducing the excitation or acquisition of the volumes smaller than the whole object. This method provides only the volume of interest without the necessity to image the surrounding tissues to avoid artifacts (such as aliasing). The main advantage of reduced FOV is considerable reduction of measurement time, enhanced resolution and improved image quality. Therefore, it allowed Gamper *et al.* to obtain 5-fold acquisition speedup and achievement of the diffusion image in a single heartbeat. This methodology was later adapted by Deux *et al.*, who used a 75% FOV and a partial k-space acquisition (87.5%) [15]. Such practice aims at reducing the time

between the excitation pulse and readout center, which limits the sensitivity of EPI to the magnetic susceptibility differences (Table II).

Navigator-gated DTI

Cardiac MRI can be performed at either end-expiration or end-inspiration. In both of these respiratory phases susceptibility artifacts can be seen (Table II), while their location is shifted towards the apex at the end-inspiration phase [16]. The end-expiration leads to a significant decrease of respiratory motion artifacts [16] and is more pronounced due to the higher reproducibility [17]. For example, in the work of Gamper *et al.*, the authors collected data for over 420 heartbeats during free breathing and chose the most frequent one for the image reconstruction based on an intensity correlation [12]. This image served as a navigator of a myocardium at the expiratory phase. Such an approach for modulus averaging was at that time a new technique for respiratory compensation alternative to breath holding [7] and synchronized breathing [10] proposed at the beginning of cardiac DTI (Table III).

The importance of this navigator-gated imaging of the heart *in vivo* was noticed by Nielles-Vallespin *et al.*, who performed reproducibility tests of these technique in comparison to the multiple breath-hold approach [18]. Both techniques showed good reproducibility of DTI parameters. Even though navigator-based measurements exhibited longer duration, lower SNR and statistically different helix angle values compared to the breath-holding technique, some of these problems can be eliminated by the development of accept/reject algorithms as stated in the work. As indicated by the authors, development of navigator-based DTI is of great importance for patients with cardiovascular disease and limited breath-holding capacity. In addition, the navigator approach, alongside the single heartbeat SE-EPI, is suitable for arrhythmic patients [17, 18].

Second- and higher-order motion compensation

Diffusion-prepared steady-state free precession

DTI techniques encoding diffusion during a single heartbeat like those presented by Gamper *et al.* [12] and Nielles-Vallespin *et al.* [19] are highly desirable, especially for clinical patients, since they allow free breathing (Table III). However, they bear a major obstacle for the achievement of the *b*-value appropriate to reach restrictions in the myocardium ($\sim$350 s mm^{-2}), which is relatively short diffusion time (tenths of the R-R interval) (Table II). This imposes the necessity of application of long diffusion gradients (10 ms for a maximum gradient of 45 mT/m [19], which is an usual maximum gradient strength available clinically), which is undesirable for cardiac applications, or relatively strong gradients not available in clinical practice (87 mT/m for a gradient duration of 8.3 ms [12]).

To address the issue of single heartbeat diffusion encoding by clinically available gradient strengths, Nguyen *et al.* developed a new diffusion-prepared pulse sequence with second order motion compensation (such as acceleration) based on steady-state free precession [20] (Table III). Briefly, the method consisted in ECG triggering, a navigator and two blocks during the diastolic quiescent phase: diffusion preparation (90° excitation pulse, two 180° refocusing pulses and a 90° tip-up pulse that stores magnetization in the longitudinal direction; four diffusion bipolar pulses that yield second order bulk motion compensation and are applied throughout the entire block, which ends up with the spoiler gradient) and the balanced steady-state free precession sequence to get image information. The advantage of the proposed sequence is the separation of diffusion encoding and the image readout. It reduces the sensitivity of the signal to T_2 relaxation, because image gradients do not contribute to *TE*, and allows the combination of different diffusion-encoding schemes with various image readouts. Moreover, it can be used for three-dimensional imaging. The study confirmed the sequence's suitability for clinical applications (weak gradients) and delivered artifact-free DW images with reasonable diffusivities in comparison to uncompensated motion sequences, which yielded highly overestimated values. However, there must be considered a trade-off between motion-compensated, single-heartbeat diffusion encoding and slightly reduced SNR due to longer *TE* = 115 ms (resulting from the diffusion preparation), while the feasibility of clinical cardiac imaging within a single heartbeat seems invaluable.

Comparison between first- and second-order motion compensation DTI

Advanced research in cardiac diffusion MRI allowed the establishment of a methodological consensus concerning the best measurement approach related to SNR, motion compensation and the optimal protocol (ECG triggering, reduced FOV, resolution, etc.) as presented above. Further development was later focused on the improvement of these issues. Having accepted that accurate DTI of the heart relies on the optimized, speeded-up SE-EPI with motion compensation and short *TE* suitable for T_2 relaxation times in the myocardium (Table II), other advanced approaches were developed in addition to the one described in section "Diffusion-prepared steady-state free precession"

Stoeck *et al.* reported such a method for the first- and second-order motion compensation based on spin echoes [21] (Tables II, III). The design of the diffusion-encoding pulse sequence relied on two bipolar gradient pulses with appropriately fitted lobe duration (while the inverted lobe is adjacent to the first lobe) for the efficient nulling of the desired gradient moment (different for the first- and second-order motion compensation), and

separated by a variable rate selective excitation (VERSE) pulse. The high gradient strength used in this study (80 mT/m) delivered $b = 450$ s mm^{-2}, which is higher than typically used (~300–350 s mm^{-2}). This suggests that the second order flow compensation can also be achieved with slightly lower gradients. However, higher gradients can provide stronger signal attenuation or its registration from tighter spaces and slower species. A significant reduction to *TE* down to 73 ms was also achieved.

In the study, several interesting observations were made when comparing first- and second-order motion compensation in DTI. First of all, in contrast to the first-order motion-compensated diffusion encoding, mean diffusivity from the second-order motion-compensated diffusion encoding proved to be insensitive to trigger delay. Moreover, it had a smaller standard deviation within the myocardium and across volunteers. Finally, the second-order motion-compensated DTI delivered physiological transmural distributions such as a linear dependency of the helix angles on the transmural depth, while no such dependency was seen with the first-order compensated DTI method. Based on these results it can be seen that the developed method for second-order motion compensation is significantly less sensitive to bulk motion, and is reproducible for different systolic phases and parts of the heart (from base to apex).

Higher-order motion-compensating diffusion gradients

The method proposed by Stoeck *et al.* for second-order motion compensation diffusion encoding, even though efficient, was tested on a high-performance gradient system [21]. As pointed out by the authors, if weaker gradients were used, they had to be longer. The increased duration of diffusion gradients results in increased sensitivity to the bulk motion deviated from the first- and second-order one. Studies providing deeper insight into the higher-order heart motion can also be found (Table III). Gradient moment nulling has been found to be simple and appropriate for the motion compensation, but for example, for each successive order of motion the number of gradient pulses is doubled, which considerably increases *TE* for the achievement of a given *b*-value [22]. It also has drawbacks connected with potential gradient waveform modifications (it works only for fixed timings).

Higher-order motion compensation pulse sequence was proposed by Welsh *et al.*, and relied on specially designed diffusion gradient waveforms (the same waveform duration, but having variable amplitudes) based on bipolar pulses placed on either side of the refocusing RF pulse [22]. The total number of gradient pulses was equal to four for acceleration (second-order) and six for jerk (third-order) compensation. In contrast, jerk-compensated diffusion encoding by gradient moment nulling via binomial expansion [21] (the same gradients' amplitude) could be provided by a total of ten pulses and would increase the required diffusion time for a given *b*-value. The proposed method was tested *in vivo* in rats and proved to be sufficient, since it delivered reliable fractional anisotropy (FA) maps and myofiber orientation. The main drawback is decreased SNR due to longer *TE*, although it is an inherent element for higher-order motion compensation requiring more gradient pulses (Table II). An indisputable advantage is the fact that the designed gradient pulse sequence can be implemented in STE. In STE attainable *b*-values can be increased from 350 to 680 s mm^{-2}. Even though the trigger delay window is narrower for SE than for STE, if the trigger delay is carefully selected, both techniques can perform similarly for compensation of motion and eddy currents [23]. Moreover, scan time can also be shortened if parallel imaging techniques are used. Following the authors, the necessary compromise among *b*-value, SNR and motion compensation can be sufficiently achieved for this approach, which offers an alternative in case of a lack of high-performance gradient hardware.

Prospects for further cardiac DTI improvements

Diffusion has been proposed as a natural biomarker for many diseases, mainly neurodegenerative [24, 25], but also musculoskeletal [26, 27] or cardiovascular [28–30]. Despite their potential, DWI and DTI indices are not used routinely in clinical practice as biomarkers of cardiovascular diseases, since they require sophisticated experimental methods as presented above. However, it was recently shown that based on standard SE-EPI, DTI is feasible for patients with acute myocardial infarction (AMI) (Table I), when sequence parameters are carefully chosen on the basis of a pilot DTI [29]. Figure 3 presents images from DTI examination of a patient with AMI, shortly after pPCI (5 days), applying the same sequence design. The results showed a very good agreement with late gadolinium enhancement images, including infarction damage zones as well as microvascular obstruction. This proves that DTI has potential to be commonly used in clinical practice for AMI patients as an alternative to gadolinium contrast agent (Table I). Hopefully, this and similar applications will be used routinely and pave the way for more advanced methods to enable accurate quantitative DTI and diffusion to become a natural biomarker of cardiovascular diseases. Although progress in cardiac DTI is clearly visible, more solutions are sought to bridge the gap between the scientific development and clinical practice.

During the cardiac DWI and DTI development many milestones have been reached, including motion compensation, achievement of the optimal *b*-value and resolution, choice of the most appropriate cardiac phase, desensitization to T_2 relaxation and SNR improvement. All

of them helped to approach accurate quantitative DWI and DTI, which in the latest papers have delivered generally reproducible values of ADCs and DTI parameters for the myocardium. It is expected that further steps will be taken to move from more common STE to SE-based DTI [31] to improve SNR without the necessity for image averaging, which may lead to erroneous diffusion tensor indices (Table II).

Another advance has been sought in diffusion tensor tractography of the myocardium. Exemplary myocardium tractography is shown in Figure 4, which was adapted from Lee *et al.* [32] and reflects three-dimensional mouse heart muscle fibers. Myocardium tractography is especially challenging in comparison to other tissues, such as nervous tissue, due to the lack of long structures in a heart muscle. Instead, it is made of syncytia of microscale cardiomyocytes. This results in the problem of the adjustment of a tract fiber length threshold, which often serves as a tool for the elimination of mistracked fibers or short tracts. The latter might appear when eigenvectors and eigenvalues have been misdetermined due to systematic errors, which leads to tracking algorithm fail. The second threshold that is important for high quality tractography is associated with anisotropy measures, such as fractional anisotropy (*FA*) [33]. However, the values of *FA* differ strongly among papers, even for healthy controls. We hypothesize that some of these differences may derive from systematic errors resulting from an inhomogeneous magnetic gradient field [34].

The recently developed *b*-matrix spatial distribution (BSD) calibration method aims at the elimination of systematic errors influencing the calculation of a diffusion tensor [35–37]. It was shown that on the grounds of the generalized Stejskal-Tanner equation [38] it is possible to accurately determine *b*-matrix, which leads to improved DTI indices and tractography [35, 37]. Moreover, the BSD approach is more straightforward in comparison to the alternative methods relying on the so-called coil tensor, *L*, obtained from the manufacturer or experimentally [39]. The method or an approach based on its simplified form has been successfully applied for living tissues, such as the brain [40, 41], skeletal muscles [27], and recently also in the myocardium [29]. In the myocardium, a noticeable improvement was observed for the *FA* value [29]. We believe that the BSD method can be applied for the enhancement of DTI in the myocardium as in other anisotropic media.

Conclusions

DWI/DTI of the human heart has been an important research target with potential clinical applications. Over the years, new developments have emerged with respect to increasing the accuracy and diagnostic value of DWI/DTI of the human heart *in vivo*. A number of applications of DTI *in vivo* and *ex vivo* have been suggested for the

characterization of myocardial structure, fiber architecture, dynamics and diseases. Progress in cardiac DTI allowed the establishment of the most suitable cardiac phase, motion compensation and diffusion weighting. Even though further developments are required in terms of *TE* shortening, acquisition time reduction, higher-order motion compensation or improved SNR, cardiac DTI is clinically feasible. This exciting research area has promising clinical relevance considering that it can deliver microstructural information and reflect the physiological status of a muscle non-invasively. Thus, DWI/DTI cardiac imaging may provide a deeper insight into macroscopic cardiac functions, empowering clinical diagnosis.

Acknowledgments

Conflict of interest

The authors declare no conflict of interest.

References

1. Tseng WYI, Wedeen VJ, Reese TG, et al. Diffusion tensor MRI of myocardial fibers and sheets: correspondence with visible cut-face texture. J Magn Reson Imaging 2003; 17: 31-42.
2. Kono K, Inoue Y, Nakayama K, et al. The role of diffusion-weighted imaging in patients with brain tumors. AJNR Am J Neuroradiol 2001; 22: 1081-8.
3. Maier SE, Sun Y, Mulkern R V. Diffusion imaging of brain tumors. NMR Biomed 2010; 23: 849-64.
4. Lanzman RS, Wittsack HJ. Diffusion tensor imaging in abdominal organs. NMR Biomed 2017; 30(3). doi:10.1002/nbm.3434.
5. Mori S, Van Zijl PCM. Fiber tracking: principles and strategies – a technical review. NMR Biomed 2002; 15: 468-80.
6. Damon BM, Froeling M, Buck AKW, et al. Skeletal muscle DT-MRI fiber tracking: rationale, data acquisition and analysis methods, applications, and future directions. NMR Biomed 2017; 30. doi:10.1002/NBM.3563.
7. Edelman RR, Gaa J, Wedeen VJ, et al. In vivo measurement of water diffusion in the human heart. Magn Reson Med 1994; 32: 423-8.
8. Legland D, Arganda-Carreras I, Andrey P. MorphoLibJ: Integrated library and plugins for mathematical morphology with ImageJ. Bioinformatics 2016; 32: 3532-4.
9. Garrido L, Wedeen VJ, Kwong KK, et al. Anisotropy of water diffusion in the myocardium of the rat. Circ Res 1994; 74: 789-93.
10. Reese TG, Weisskoff RM, Smith RN, et al. Imaging myocardial fiber architecture in vivo with magnetic resonance. Magn Reson Med 1995; 34: 786-91.
11. Tseng WYI, Reese TG, Weisskoff RM, Wedeen VJ. Cardiac diffusion tensor MRI in vivo without strain correction. Magn Reson Med 1999; 42: 393-403.
12. Gamper U, Boesiger P, Kozerke S. Diffusion imaging of the in vivo heart using spin echoes-considerations on bulk motion sensitivity. Magn Reson Med 2007; 57: 331-7.

13. Dou J, Reese TG, Tseng WYI, Wedeen VJ. Cardiac diffusion MRI without motion effects. Magn Reson Med 2002; 48: 105-14.

14. Feinberg DA, Hoenninger JC, Crooks LE, et al. Inner volume MR imaging: technical concepts and their application. Radiology 1985; 156: 743-7.

15. Deux JF, Maatouk M, Vignaud A, et al. Diffusion-weighted echo planar imaging in patients with recent myocardial infarction. Eur Radiol 2011; 21: 46-53.

16. Vu KN, Haldipur AG, Roh ATH, et al. Comparison of end-expiration versus end-inspiration breath-holds with respect to respiratory motion artifacts on T1-weighted abdominal MRI. Am J Roentgenol 2019; 212: 1024-9.

17. Taylor AM, Jhooti P, Wiesmann F, et al. MR navigator-echo monitoring of temporal changes in diaphragm position: implications for MR coronary angiography. J Magn Reson Imaging 1997; 7: 629-36.

18. Nielles-Vallespin S, Mekkaoui C, Gatehouse P, et al. In vivo diffusion tensor MRI of the human heart: Reproducibility of breath-hold and navigator-based approaches. Magn Reson Med 2013; 70: 454-65.

19. Nielles-Vallespin S, Mekkaoui C, Gatehouse P, et al. In vivo diffusion tensor mri of the human heart: reproducibility of breath-hold and navigator-based approaches. Magn Reson Med 2013; 70: 454-65.

20. Nguyen C, Fan Z, Sharif B, et al. In vivo three-dimensional high resolution cardiac diffusion-weighted MRI: a motion compensated diffusion-prepared balanced steady-state free precession approach. Magn Reson Med 2014; 72: 1257-67.

21. Stoeck CT, Von Deuster C, GeneTM, et al. Second-order motion-compensated spin echo diffusion tensor imaging of the human heart. Magn Reson Med 2016; 75: 1669-76.

22. Welsh CL, DiBella EVR, Hsu EW. Higher-order motion-compensation for in vivo cardiac diffusion tensor imaging in rats. IEEE Trans Med Imaging 2015; 34: 1843-53.

23. Stoeck CT, von Deuster C, van Gorkum RJH, Kozerke S. Motion and eddy current-induced signal dephasing in in vivo cardiac DTI. Magn Reson Med 2020; 84: 277-88.

24. Kamagata K, Andica C, Kato A, et al. Diffusion magnetic resonance imaging-based biomarkers for neurodegenerative diseases. Int J Mol Sci 2021; 22: 5216.

25. Andica C, Kamagata K, Hatano T, et al. MR biomarkers of degenerative brain disorders derived from diffusion imaging. J Magn Reson Imaging 2020; 52: 1620-36.

26. Zaraiskaya T, Kumbhare D, Noseworthy MD. Diffusion tensor imaging in evaluation of human skeletal muscle injury. J Magn Reson Imaging 2006; 24: 402-8.

27. Mazur W, Urbańczyk-Zawadzka M, Banyś R, et al. Diffusion as a natural contrast in MR imaging of peripheral artery disease (PAD) tissue changes. A case study of the clinical application of DTI for a patient with chronic calf muscles ischemia. Diagnostics 2021; 11: 92.

28. Khalique Z, Ferreira PF, Scott AD, et al. Diffusion Tensor cardiovascular magnetic resonance in cardiac amyloidosis. Circ Cardiovasc Imaging 2020; 13: 9901.

29. Mazur W, Urbańczyk-Zawadzka M, Czyż Ł, et al. Diffusion-tensor magnetic resonance imaging of the human heart in health and in acute myocardial infarction using diffusion-weighted echo-planar imaging technique with spin-echo signals. Adv Interv Cardiol 2022; 18: 416-22.

30. Wu MT, Tseng WYI, Su MYM, et al. Diffusion tensor magnetic resonance imaging mapping the fiber architecture remodeling in human myocardium after infarction: correlation with viability and wall motion. Circulation 2006; 114: 1036-45.

31. Mekkaoui C, Reese TG, Jackowski MP, et al. Diffusion MRI in the heart. NMR Biomed 2017; 30: e3426.

32. Lee SE, Nguyen C, Yoon J, et al. Three-dimensional cardiomyocytes structure revealed by diffusion tensor imaging and its validation using a tissue-clearing technique. Sci Rep 2018; 8: 6640.

33. Nielles-Vallespin S, Scott A, Ferreira P, et al. Cardiac diffusion: technique and practical applications. J Magn Reson Imaging 2020; 52: 348-68.

34. Sang-eun Lee. Three-dimensional Cardiomyocytes Structure Revealed by Diffusion Tensor Imaging and Its Validation Using a Tissue-Clearing Technique. Springer Nature 2018.

35. Borkowski K, Krzyżak AT. Analysis and correction of errors in DTI-based tractography due to diffusion gradient inhomogeneity. J Magn Reson 2018; 296: 5-11.

36. Krzyżak AT, Olejniczak Z. Improving the accuracy of PGSE DTI experiments using the spatial distribution of b matrix. Magn Reson Imaging 2015; 33: 286-95.

37. Borkowski K, Krzyżak AT. Assessment of the systematic errors caused by diffusion gradient inhomogeneity in DTI-computer simulations. NMR Biomed 2019; 32: 1-12.

38. Borkowski K, Tadeusz A. The generalized Stejskal-Tanner equation for non-uniform magnetic field gradients. J Magn Reson 2018; 296: 23-8.

39. Hansen CB, Rogers BP, Schilling KG, et al. Empirical field mapping for gradient nonlinearity correction of multi-site diffusion weighted MRI. Magn Reson Imaging 2021; 76: 69-78.

40. Obuchowicz R, Krzyżak AT. Improvement of brain tractography using the BSD-DTI method on the example of subcortical u-fibers visualization. European Congress of Radiology 2019: C-1975. doi:10.26044/ecr2019/C-1975.

41. Lee Y, Kettinger AO, Jakob B, et al. A comprehensive approach for correcting voxel-wise b-value errors in diffusion MRI. Magn Reson Med 2020; 83: 2173-84.